NASA TN D-277

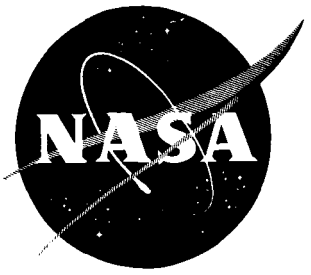

TECHNICAL NOTE

D-277

APPLICATION OF VARIOUS TECHNIQUES FOR DETERMINING LOCAL HEAT-TRANSFER COEFFICIENTS IN A ROCKET ENGINE FROM TRANSIENT EXPERIMENTAL DATA

By Curt H. Liebert, James E. Hatch, and Ronald W. Grant

Lewis Research Center
Cleveland, Ohio

NATIONAL AERONAUTICS AND SPACE ADMINISTRATION

WASHINGTON

April 1960

NATIONAL AERONAUTICS AND SPACE ADMINISTRATION

TECHNICAL NOTE D-277

APPLICATION OF VARIOUS TECHNIQUES FOR DETERMINING LOCAL HEAT-TRANSFER COEFFICIENTS IN A ROCKET ENGINE FROM TRANSIENT EXPERIMENTAL DATA

By Curt H. Liebert, James E. Hatch, and Ronald W. Grant

SUMMARY

The design of rocket engines is based on knowledge of the local values of heat-transfer coefficient. One of the more attractive experimental methods for gaining gas-side heat-transfer coefficients is by transient heat-transfer measurement in a solid-wall, heat-capacitance rocket engine. This technique obviates some of the instrumentation difficulties that would be encountered if a liquid-cooled engine were used to measure local steady-state heat-transfer data.

The transient heat-transfer data obtained from a thermal-capacitance rocket can be analyzed by a number of methods. These vary in complexity from approximate methods to rather complex solutions of the partial differential equations of unsteady heat conduction. Six analytical techniques for determining heat-transfer coefficients from transient experimental data are discussed and applied to obtain local values of heat-transfer coefficients in an ammonia-oxygen rocket. The integration method appears to be the best of the six from the standpoint of possible accuracy in the determination of local heat-transfer coefficients.

INTRODUCTION

The design of rocket engines necessitates obtaining local gas-side experimental heat-transfer coefficients in order to determine the validity of empirical methods of calculating heat-transfer coefficients.

Heat transfer can be measured in a rocket engine by either steady-state or transient techniques. To obtain steady-state conditions in a rocket motor whose gas temperature is above the melting point of the metal, the walls must be cooled. This type of engine presents instrumentation difficulties in that generally the coolant passages are small

and the passage walls are thin. Transient heat-transfer data may be obtained from solid-wall rocket engines. For short running times, no cooling is required if the solid walls are of proper material to act as heat sinks.

Equations for turbulent flow in tubes indicate that the heat-transfer coefficient is a function of the propellant properties based on film temperature, flow area, and propellant flow. The heat-transfer coefficient varies significantly during the starting transient of a rocket motor because of the variations in chamber pressure and propellant flow. The coefficient should, however, reach a quasi-steady-state value soon after constant propellant flow and constant chamber pressure have been established and vary thereafter only as a result of changing property values due to changing film temperature.

The observed rates of temperature rise through the walls of a thermal-capacitance rocket engine can be analyzed by a number of methods, such as given in references 1 and 2. For this investigation, time-temperature data were obtained from copper plugs installed in an ammonia-oxygen rocket. Local values of heat-transfer coefficient were calculated from six selected methods. These methods vary in complexity from approximate methods to rather complex solutions of the partial differential equations of unsteady heat conduction. The resulting heat-transfer coefficients, as well as an evaluation of each of the six methods based on estimated accuracy, ease of calculation, and applicability, are presented herein.

APPARATUS AND EXPERIMENTAL PROCEDURE

A 2400-pound-thrust, solid-wall, ammonia-oxygen rocket was used in the experiments to obtain transient temperature data. A small copper plug was devised which, when inserted in the wall of an uncooled rocket engine, would approximate a one-dimensional finite slab. Under these conditions, the local transient rate of heat transfer and the local heat-transfer coefficient may be calculated from measured temperature distributions within the element. The element had to be rugged in construction in order to withstand the high temperatures and pressures within the chemical rocket.

As shown in figures 1 and 2, tapered holes with a 39° included angle were machined through the entire wall of the mild steel chamber and through the copper nozzle at the throat. Rods of pure copper with diameters of 0.6055 and 0.265 inch were used in the chamber and throat, respectively. Copper was selected because its high thermal diffusivity would delay the temperature rise at its heated surface. The plugs were machined with a 0.005-inch by 39° taper to enable them to seize in the

small diameter of the hole, but with a small contact area between the plug and wall in order to minimize conduction between the plugs and the chamber. The heat-transfer surfaces of the plugs were machined to the contour of the chamber and nozzle throat.

Figure 1 shows the thermocouple stations on the copper plug. Nine Chromel-Alumel thermocouples were used: two groups of four thermocouples, each group located circumferentially 180° apart with equal axial spacing, and one thermocouple on the cold end of the plug. The Chromel and Alumel wires 0.008 inch in diameter were separately peened to the surface in a plane perpendicular to the plug axis, the distance between being about 1/64 inch. The position of the thermocouples on the copper plug in the throat of the nozzle is shown in figure 2.

Sauereisen cement was placed in the gap between the plugs and the wall. The sauereisen was used to keep heat conduction between the copper plug and the chamber wall to a minimum to insure local one-dimensional heat conduction. The plugs were held in place by a steel cover in contact with the end of the plug. The cover was attached to the rocket wall by screws.

The rocket engine was installed on a thrust stand. Propellant flow, chamber pressure, oxidant-fuel ratio, and thrust were measured for the evaluation of performance. The transient temperature data obtained from the thermocouples were recorded with an oscillograph.

For the purpose of checking out the experimental procedure and instrumentation with a limited number of instrument channels, the transient heat transfer in the chamber and in the nozzle was tested separately.

PRESENTATION OF DATA

Experimental heat-transfer data from a plug located in the chamber and one located in the nozzle throat are presented herein. These data are employed in the various analytical methods for computing heat-transfer coefficients, as discussed in the next section.

The variation of chamber pressure with time for the two tests is presented in figure 3. The steady-state chamber pressure and oxidant-fuel ratio for the chamber test were approximately 513 pounds per square inch absolute and 1.258, respectively. The combustion temperature was estimated by multiplying the theoretical temperature at a chamber pressure of 600 pounds per square inch absolute and an oxidant-fuel ratio of 1.258 (ref. 3) by the square of the ratio of the experimental to the theoretical characteristic velocities. Because of the low gas velocity in the chamber the temperature so determined, 3816° F, was considered to be the recovery temperature.

The steady-state chamber pressure and oxidant-fuel ratio for the throat test were approximately 474 pounds per square inch absolute and 1.347, respectively. The theoretical combustion temperature t_t and theoretical static temperature t_s at the throat were calculated from reference 3 as just described, assuming equilibrium composition during isentropic expansion. (All symbols are defined in the appendix, p. 19). The recovery temperature of 3285° F at the throat was computed from $t_r = (t_t - t_s)r + t_s$, where r (recovery factor) was taken as 0.90. This value of r was determined from a plot of r against Reynolds number for flow along a cylinder given in reference 4.

The temperature data against time from the start of propellant injection for the chamber test are shown in figure 4. At the start of the test there was a 13° F variation along the length of the plug. After approximately 0.9 second, the temperatures at all points in the plug rose in an orderly fashion. The pressure plots of figure 3 indicate that combustion pressure had stabilized after 0.9 second. After 1.4 seconds, the temperature rise for all thermocouples was approximately linear, and the maximum temperature difference between any two thermocouples at the same radial distance from the heat-transfer surface was about 15° F. This difference became smaller as the distance from the heat-transfer surface increased. For this run the slope of the temperature-time curves was about the same at 0.25, 0.375, and 0.500 inch from the heated end. Thermocouple number 1 was inoperative at the start of the run.

A crossplot of temperature against distance at various times is shown in figure 5 for the chamber test. The fact that $\partial t/\partial x \neq 0$ at the cold end indicates some heat transfer at this point. The vertical line at 41 percent of plug length from the heated surface indicates the point in the plug having approximately the average temperature.

In general, a wall temperature is necessary for the calculation of the surface coefficient of heat transfer h. A thermocouple was not mounted on the heat-transfer surface because of the resultant error in measured temperature due to the large temperature gradient across the area of the thermocouple. Thus, the thermocouples were mounted as shown in figures 1 and 2, and the wall temperatures were obtained from a plot on semilog paper of plug temperature against distance as shown in figure 6. It is noteworthy that on this type of plot the lines were quite linear near the heat-transfer surface and thus lent themselves to a more reliable extraploation for the wall temperature. The wall temperatures shown in figures 4 and 5 were determined from figure 6.

The variation of plug temperature with time from the start of propellant flow for the throat test is presented in figure 7. The variation of plug temperature at the start of the run was approximately 35° F.

After approximately 0.9 second the plug temperatures rose in an orderly fashion. This indicates that the starting transient was over, as verified by figure 3. Wall temperatures in figure 7 were determined by means of a straight-line extrapolation through the two innermost temperature readings on a semilog plot similar to figure 6. The distribution of temperature with distance is shown in figure 8.

DISCUSSION OF METHODS

The following six methods (referred to herein as methods I to VI) for the determination of one-dimensional transient heat flow are discussed generally. In all calculations it is assumed that radiation heat transfer to the plugs is negligible.

I: Integration Method

If the plug is considered to be insulated on all surfaces except the heat-transfer surface and the cold end of the plug, the time rate of change of the integrated heat content must be equal to the rate of heat flow through the surfaces:

$$\dot{q} = \frac{1}{A}\frac{\partial}{\partial\theta}\int_0^L A_x Q_x \, dx + k\left(\frac{\partial t}{\partial x}\right)_0 = \frac{1}{A}\frac{\partial}{\partial\theta}\int_0^L (\rho A c t)_x \, dx + k\left(\frac{\partial t}{\partial x}\right)_0 \tag{1a}$$

The heat loss from the cold end is accounted for by $k\left(\frac{\partial t}{\partial x}\right)_0$. This heat loss may be minimized by insulating the cold end of the plug. In equation (1a), the heat content Q_x is above some arbitrary reference level. If the plug cross-sectional area is constant over its length, the area term does not appear in equation (1a). If a short time increment after the start of steady-state burning is considered, the time rate of change of integrated heat content at the arithmetic average of these two times is equal to the difference in heat content divided by the time interval. Or, for a constant-area plug with heat loss from the cold end, equation (1a) may be written as

$$\dot{q}_{\frac{1}{2}(\theta_1+\theta_2)} = \frac{1}{\theta_2 - \theta_1}\left[\int_0^L (\rho c t)_{\theta_2} \, dx - \int_0^L (\rho c t)_{\theta_1} \, dx\right]$$

(2)

Equation (1b) may be used to obtain the heat flux. The heat-transfer coefficient can be obtained from the following equation:

$$h_{\frac{1}{2}(\theta_1+\theta_2)} = \frac{1}{t_r - t_{w,\frac{1}{2}(\theta_1+\theta_2)}} \left\{ \frac{1}{\theta_2 - \theta_1} \left[\int_0^L (\rho c t)_{\theta_2} \, dx - \int_0^L (\rho c t)_{\theta_1} \, dx \right] + k\left(\frac{\partial t}{\partial x}\right)_{0,\frac{1}{2}(\theta_1+\theta_2)} \right\} \qquad (2a)$$

In this equation the ρc product is evaluated at the measured temperature at x, and k is evaluated at the temperature of the cold end. In the following discussion, the value of h obtained by neglecting the cold-end heat loss is calculated by

$$h_{\frac{1}{2}(\theta_1+\theta_2)} = \frac{1}{t_r - t_{w,\frac{1}{2}(\theta_1+\theta_2)}} \left\{ \frac{1}{\theta_2 - \theta_1} \left[\int_0^L (\rho c t)_{\theta_2} \, dx - \int_0^L (\rho c t)_{\theta_1} \, dx \right] \right\} \qquad (2b)$$

Heat-transfer coefficients for the chamber and throat plugs were obtained by plotting ρct against distance and mechanically integrating the area between θ_1 and θ_2 in order to obtain a value neglecting heat loss out of the cold end (eq. (2b)). The heat loss from the cold end was then approximated from figures 5 and 8 and used in equation (2a) to obtain the total h. For the chamber plug the time intervals of 1.2 to 1.80, 1.2 to 2.45, and 1.8 to 2.45 seconds were used to obtain values of h at 1.50, 1.825, and 2.125 seconds, respectively. For the throat plug the time intervals of 1.00 to 1.80, 1.00 to 2.72, 1.80 to 2.72, and 2.3 to 2.72 seconds were used to obtain values of h at 1.40, 1.86, 2.26, and 2.51 seconds, respectively.

II: Constant h Method

Reference 5 presents curves of $(t_x - t_o)/(t_r - t_o)$ plotted against hL/k with $\alpha\theta/L^2$ as a parameter for fixed values of x/L where x is measured from the heated surface. The curves were obtained by solving the transient heat-flow equation in difference form using a fine-grid spacing on a high-speed computing machine for several hL/k values (assuming constant h and t_r). In order to use these curves, the material

properties (k, ρ, and c) should be evaluated at $\bar{t} = (t_w - t_o)/4 + t_o$ at the time of reading t_x. According to Storm (ref. 6) this temperature $\bar{t}$ gives a good approximation to the solution of the nonlinear equation for simple metals. To evaluate properties, t_w may be approximated as a first trial; and, after hL/k has been determined, t_w may be found. Thus, the $\bar{t}$ values may be obtained by an iteration procedure. After these material properties are evaluated, it is possible to calculate $(t_x - t_o)/(t_r - t_o)$ and $\alpha\theta/L^2$ from one temperature reading and to find hL/k by using the appropriate x/L family of curves. The values of h may then be determined from this parameter.

III: Cresci-Libby Method

Carslaw and Jaeger (ref. 2) solved the general one-dimensional partial differential equation of transient heat conduction,

$$\frac{\partial t}{\partial \theta} = \frac{k}{\rho c}\left(\frac{\partial^2 t}{\partial x^2}\right) \tag{3}$$

for a finite slab with arbitrary surface-temperature distribution and constant diffusivity by imposing the following boundary conditions on this equation:

$t = t_o$ at $\theta = 0$

$t = t_o + \varphi(\theta)$ at $x = L$ (x measured from unheated surface)

$\partial t/\partial x = 0$ at $x = 0$

The resultant temperature distribution is given by

$$t(x,\theta) = t_o + \frac{2}{L}\sum_{n=0}^{\infty} e^{-\alpha\beta_n^2\theta} \cos \beta_n x \left[(-1)^n \alpha\beta_n \int_0^{\theta} e^{\alpha\beta_n^2\lambda}\, \varphi(\lambda)\, d\lambda\right] \tag{4}$$

where

$$\beta_n = \frac{(2n + 1)\pi}{2L}$$

To obtain $\dot{q}$ at the surface, this equation first must be differentiated with respect to θ, and then the resultant expression may be

integrated with respect to x in the heat-conduction equation:

$$\dot{q}_{x=L} = \int_0^L \rho c \left(\frac{\partial t}{\partial \theta}\right) dx$$

With this procedure, the expression for $\dot{q}_{x=L}$ becomes (ref. 7)

$$\dot{q}_{x=L} = \frac{2k}{L} \sum_{n=0}^{\infty} \left[\varphi(\theta) - \beta_n^2 \alpha \int_0^{\theta} \varphi(\lambda) e^{-\beta_n^2 \alpha (\theta - \lambda)} \, d\lambda \right] \tag{5}$$

From a given wall-temperature distribution, $\dot{q}_{x=L}$ may then be evaluated and h computed from $h = \dfrac{\dot{q}_{x=L}}{t_r - t_w}$.

A smooth curve drawn through the extrapolated surface-temperature distribution for both chamber and throat conditions was found to be approximated by a quadratic equation for the form $t_w = a\theta^2 + b\theta + c$ when the rocket had achieved steady chamber pressure conditions. The curve fit the wall temperature distribution within $\pm 10^{\circ}$ F. However, it was not possible to fit the quadratic equation to the wall temperature distribution when the chamber pressure was rising.

The equations $\varphi(\theta) = a\theta^2 + b\theta$ and $\varphi(\lambda) = a\lambda^2 + b\lambda$ were substituted into equation (5), and $\dot{q}$ and h were evaluated at a given burning time. The infinite sum was evaluated for eight terms. This was enough to approximate the answer with a good degree of accuracy, since the last term was less than 0.5 percent of the sum of the previous terms.

The equation $\varphi(\lambda) = a\lambda^2 + b\lambda$ was also substituted into equation (4) to see how well the predicted temperature anywhere within the plug at any time would match the experimental conditions. The analytical expression predicted the temperature at 0.5 inch from the heat-transfer surface and at a burning time of 2.3 seconds within 2 percent of the experimental data after eight terms were calculated in the infinite sum. This agreement of theory and experiment verifies the assumption of one-dimensional heat flux and indicates that the instrumentation was reasonably accurate.

IV: Numerical Method

Max Jakob (ref. 8) suggests a numerical method to solve linear unsteady-state conduction problems in a rod by following Dusinberre's procedure. The Dusinberre procedure applies to a rod that has been divided into volume increments by planes perpendicular to the one-dimensional heat flow. This method is essentially an application of a finite-difference-type solution using a very coarse grid spacing. In this respect the method is similar to method II (constant h). The temperature at the center of each increment is assumed to be the representative temperature of the increment at time θ. At a surface where convection occurs, an arrangement such as shown in figure 9 may be used. The heat balance for the half-block $\Delta x/2$ becomes

$$hA(t_r - t_w)\Delta\theta + \frac{kA}{\Delta x}(t_1 - t_w)\Delta\theta = \rho cA\frac{\Delta x}{2}(t_{w,\Delta\theta} - t_w) \qquad (6)$$

where $t_{w,\Delta\theta}$ is evaluated after a small time interval $\Delta\theta$.

In order to apply the heat-balance equation, equation (6) was modified to incorporate a finite slab. In equation (6) the term $\rho cA(\Delta x/2)(t_{w,\Delta\theta} - t_w)$ was used to describe the heat absorbed by a very thin slab. Since a finite slab is being considered in this application, it is more reasonable to incorporate the average temperature of the half-block $t_{a,\Delta\theta}$ ($\Delta x/2$ in fig. 9). Thus, equation (6) becomes

$$hA(t_r - t_w)\Delta\theta + k\frac{A}{\Delta x}(t_1 - t_w)\Delta\theta = \frac{\rho cA\,\Delta x}{2}(t_{a,\Delta\theta} - t_a) \qquad (7)$$

In equation (7), Δx is two-thirds of the plug length and $\Delta\theta$ was evaluated at a time interval of 0.2 second. The values ρ and c were evaluated at the average temperature of $t_{a,\Delta\theta}$ and t_a, while k was evaluated at the average temperature of t_1 and t_w.

V: Greenfield Method

The Greenfield method (ref. 9) considers a rocket wall as a thermal capacitor. It is a technique that may be applied herein for determination of the heat transferred from the combustion gases through the gas film to the surface of the copper plug. The transient heat transfer may be determined from

$$\dot{q} = \frac{Wc}{A}\left(\frac{\partial t}{\partial\theta}\right)_a \qquad (8)$$

where $(\partial t/\partial\theta)_a$ is the rate of change of average plug temperature with respect to time. The heat-transfer coefficient may be expressed by

$$h = \frac{\dot{q}}{t_r - t_w} \tag{9}$$

This method is an approximation to method I (integration). The similarity may be seen by rewriting equation (1) and neglecting heat loss from the cold end of the plug:

$$q_{\frac{1}{2}(\theta_1+\theta_2)} = \frac{1}{\theta_2 - \theta_1}\left[\int_0^L (\rho ct)_{\theta_2}\,dx - \int_0^L (\rho ct)_{\theta_1}\,dx\right]$$

By assuming ρ and c to be constant and t to be a mean temperature at times θ_1 and θ_2, the equation becomes

$$\dot{q} = \rho cx\,\frac{t_{\theta_2} - t_{\theta_1}}{\theta_2 - \theta_1} = \frac{Wc}{A}\left(\frac{\Delta t}{\Delta\theta}\right)_a$$

where

$$\frac{W}{Ax} = \rho$$

The average temperature of the chamber plug occurred at 41 percent of the plug length or 0.427 inch measured from the heated end (fig. 5). This distance was determined graphically by integrating under each curve of t against x from 1.2 to 2.45 seconds. The slope of the average plug temperature $(dt/d\theta)_a$ was determined graphically from figures 4 and 7 at about 41 percent of the plug length. The specific heat of the plug was evaluated at the average temperature and substituted into equations (8) and (9) along with t_r, t_w, and the plug geometry.

VI: Semilog Extrapolation Method

Since four of the previous solutions require an extrapolation to obtain t_w in order to evaluate h, the possibility arises of evaluating h by this extrapolation. Plotting the data as log t against x measured from the heated surface indicated that within the limit of scatter a straight line could be drawn through the temperature readings in most cases (fig. 6). If this linearity is assumed to hold to the wall, both t_w and $(\partial t/\partial x)_w$ may be found. The results then may be

substituted in the following equation for h:

$$h = \frac{kt_w \frac{\partial(\log t)}{\partial x}}{t_r - t_w} \tag{10}$$

RESULTS

Figures 10 and 11 present the variation of transient heat-transfer coefficient with burning time in the chamber and at the throat as computed from the transient experimental data by the six selected methods. The heat-transfer coefficients were evaluated during the range of burning times where the chamber pressure and propellant flow were relatively constant. If the common assumption is made that the thermal boundary layer adjusts instantaneously to the changes in wall temperature, these values of h may be interpreted to be the quasi-steady-state values at their corresponding experimental wall temperatures.

Table I shows the values of h in the chamber and at the throat for burning times of 2.1 and 2.5 seconds, respectively. These values were obtained from figures 10 and 11. The percent variation of the methods from the integration method, equation (2a), is also given. The results were compared with the integration method because, as is made clear in ANALYSIS OF METHODS, it is considered to be the most adaptable to the experimental conditions. For most engineering purposes an accuracy of ±20 percent may be considered as adequate.

The heat-transfer coefficient as calculated by method I (integration), equation (2a), which assumes h may vary with wall temperature, shows a 1-percent variation of h in the chamber during a burning time of 0.62 second (fig. 10). Also shown is a 11-percent variation in h at the throat during a burning time of 1.11 seconds (fig. 11). The variations in wall temperature were about 125° and 248° F, respectively. Thus, the variation of h with time may be considered small for the full flow duration of these tests.

Appreciable variations of h may occur, however, during the starting transient when chamber pressure and gas temperature vary widely.

If the heat loss from the cold end of the plug is neglected, the heat-transfer coefficient obtained by equation (2b) is lower than the results given by equation (2a), as indicated in figures 10 and 11. For the times considered in table I, this heat loss was 9 percent in the chamber and 12 percent in the throat. Correspondingly, the heat-transfer coefficients computed by equation (2b) were 9 and 12 percent lower than those given by equation (2a) for the chamber and throat, respectively.

Figures 10 and 11 show that method II (constant h) gives relatively good agreement with method I, equation (2a), for both tests over a range of burning times. In these computations of h by method II the time increment θ was taken from the initiation of propellant flow to the time at which h was evaluated. Table I and figure 10 indicate that method II agrees well in the chamber and is 12 percent low in the throat when compared with equation (2a). Considering the simplicity of application of method II, this agreement with the integration method is considered relatively good even though certain assumptions made in the solution of this method are not applicable to the test conditions. These assumptions are that the free-stream temperature and h will be constant over the duration of time θ. Also, there must be no heat loss from the plug. Figure 3 shows that for the chamber test the chamber pressure was constant after about 1 second of burning time. Thus, during the transition period from the initiation of propellant flow to 1 second the combustion temperature and h were varying greatly. Also, a comparison of equations (2a) and (2b) in table I for the chamber indicates an appreciable heat loss from the cold end of the plug. For the chamber tests these factors appear to be compensating because of the good agreement of method II with method I.

An accurate evaluation of time θ is required in the application of method II. Figures 3 and 4 for the chamber test show that the wall temperature started to increase rapidly at the start of propellant flow. However, figures 3 and 7 for the throat test indicate that the wall temperature did not rise as rapidly at the initiation of propellant flow. A temperature extrapolation to the initial temperature of the thermocouple closest to the heated surface indicates that rapid combustion did not start until about 0.6 second after the initiation of propellant flow. This ignition delay is indicated by the dashed line in figure 7. By starting θ at 0.6 second after the initiation of propellant flow, the numerical agreement of this method with method I becomes better at the throat, as seen in table I. The temperature extrapolation in the chamber is coincident with the initiation of propellant flow, as seen by figure 3 and the dashed line in figure 4. Thus, seemingly better numerical agreement of method II with method I was achieved for these data in both chamber and throat by use of the temperature-time extrapolation. Method II is expected to be good for cases where the ignition delay and starting transients are small compared with total burning time and where the cold end of the plug is insulated.

Table I and figures 10 and 11 show that the values calculated by method III (Cresci-Libby) are near agreement with method I, equation (2a), near the end of burning for both tests. Method III is 16 percent high in the chamber and 7 percent low in the throat. The heat-transfer coefficient more closely approaches the value of h computed with method I, equation (2a), as the burning time is increased; this reflects the

sensitivity of this method toward the starting transient. The heat-transfer coefficient shows no tendency to level off near the end of burning. This is probably due to the difficulty of calculating a curve to fit exactly the plot of surface temperature against burning time, especially at the start of burning.

Method IV (numerical) and method V (Greenfield) agree well with method I, equation (2a), near the end of burning for both tests as indicated by table I and figures 10 and 11. Method IV is 7 percent high in the chamber and 2 percent high at the throat. Method V is 2 percent low in the chamber and 7 percent low at the throat. The results of these methods in general approach more closely the values obtained by method I, equation (2a), as the burning time is increased. These methods also show a general leveling off of h near the end of burning time, indicating that the effect of the starting transient is less appreciable.

Method VI (semilog extrapolation) gives appreciable variations of h with burning time, as indicated in figures 10 and 11. The scatter of h with burning time is primarily due to lack of accuracy in the determination of the slope and wall temperature. Small errors in the determination of the slope and temperature values at the wall result in relatively large errors in the calculated values of h.

It is suggested in the literature that the rocket-motor designer use the Colburn equation, reference 10, as a possible method for estimating the gas-side heat-transfer coefficient. It is also recommended in the literature that all gas properties in the Colburn equation be evaluated at a film temperature when applications involve large Reynolds numbers and Δt. The film temperature is evaluated as the average of the static temperature and the wall temperature.

The variations of h with burning time computed by the Colburn equation are plotted in figure 12 for both runs. The results show a 2-percent variation in h in the chamber during a 1.05-second burning time at constant pressure and a 4-percent variation in h at the throat during a burning time of 1.52 seconds at constant pressure. This small variation of h with burning time is in agreement with the results obtained with method I, equation (2a). The absolute values of h also agree within engineering accuracy with method I in the chamber and at the throat. Inasmuch as large axial and circumferential variations of heat flux have been observed in studies of solid-wall and regenerative engines, this agreement of the values of h may be fortuitous. More extensive investigations of the type reported herein are required to establish whether or not the Colburn equation can predict heat-transfer coefficients in rocket engines with a sufficient degree of accuracy.

ANALYSIS OF METHODS

In this section a short analysis of the applicability of each transient method is discussed.

Method I

The integration method provides the best means of calculating h when burning times are short, provided the variations of h are continuous and of not too great a magnitude. If the time increment is taken after the start of steady-state combustion, the effect of the starting transient is generally eliminated. Only a short period of combustion is necessary to obtain a value of heat-transfer coefficient. This method allows for correction of heat losses from the cold end of the plug if such losses exist. There is no doubt about the temperature at which to evaluate the plug-material properties (ρ, c, and k), and their variation with temperature is accounted for (nonlinear case) within the accuracy to which the properties are known. The largest error is expected to arise in obtaining the hot wall temperature. The wall temperature can be either measured directly, or a sufficiently accurate extrapolation may be obtained from a plot of log t against x through the inner points. In obtaining heat-transfer coefficients, the error in wall temperature appears in the form of $t_r - t_w$. This quantity is usually larger than t_w, so that a certain percentage error in t_w represents a much smaller percentage error in heat-transfer coefficient. Concerning method I, it may be stated that:

(1) Several thermocouples are needed to determine $t = f(x)$ and t_w with reasonable accuracy.

(2) The solution is reasonably easy to obtain and contains only minor approximations.

(3) If heat loss from the cold end of the plug occurs, it may be accounted for - at least approximately.

(4) The results should be accurate as soon as stable burning is achieved. The time interval used for the integration should be long enough that inaccuracies of the interval do not become appreciable, but not so long that the mean-time approximation is greatly in error.

Method II

The constant h method makes use of the solution of the linear heat-flow equation but in a dimensionless form. With this method it must

be assumed that the combustion temperature, heat-transfer coefficient, and material properties are invariant with burning time. Furthermore, the time increment over which h and t are applied must be evaluated. The accuracy of the results depends on how nearly these assumptions are satisfied. This method should be good for cases where the burning time is long compared with the duration of the starting transient. For short running times and adverse starting transient conditions, fairly accurate approximations of h may be obtained by starting θ from the estimated time at which the wall temperature starts to increase rapidly. The following statements may be made concerning method II:

(1) Only one thermocouple, from which a reading is taken at an accurately determined time from the start of heat addition, is needed.

(2) Since curves can be used to determine h, the reduction of data is very simple.

(3) The plug temperature must be essentially uniform at the start of heat addition.

Method III

The Cresci-Libby method is a very rigorous mathematical approach to the solution of the linear heat-transfer equation. The reliability of the results is influenced by the accuracy with which t_w can be determined and with which $t_w = f(\theta)$ can be expressed by an equation over the whole period of running. The curve of t_w and time is very difficult to fit during the starting transient, and thus there may be an error due to this transient. How near the assumption of constant material properties approximates the actual case is also open to some question. The following statements may be made about method III:

(1) The plug temperature must be essentially uniform at the start of heat addition.

(2) Several thermocouples are needed to obtain an approximate wall temperature unless a thermocouple can be located on the heat-transfer surface of the plug.

(3) The results are dependent on how well $t_w = f(\theta)$ can be expressed.

(4) The equation for $\dot{q}$ from which h is obtained is relatively difficult to solve.

Method IV

The numerical method, as used in the present application, assumes that dt/dx at the point one-third of the distance from the hot end of the plug is represented by the difference in the temperature at the point two-thirds of the distance from the hot end and the heated wall divided by $2L/3$. It also assumes that the time rate of change of the center of the inner one-third of the plug represents the time rate of change of this whole segment. The method is essentially an application of a finite-difference-type solution using a very coarse grid spacing. The accuracy of these assumptions obviously is greatly dependent on the shape of the curves of $t = f(x)$ and $t = f(\theta)$. The accuracy is also not as good as method II because of the coarser grid spacing used herein. The following statements may be made about method IV:

(1) Several thermocouples are needed to determine an approximate wall temperature by extrapolation unless a thermocouple can be located exactly on the heat-transfer surface of the plug.

(2) Although this method furnishes numbers that are in fairly good agreement with more rigorous methods in this case, there is no assurance that this would always be the case because of the assumptions involved.

Method V

The Greenfield method furnishes a means of determining h by assuming that at some time the time rate of change of temperature at a single point in the plug divided by the difference between gas-recovery temperature and wall temperature is proportional to the heat-transfer coefficient. However, this is true only at one time for this particular thermocouple location. The results indicated that, when the temperature reading 41 percent of the way from the hot end is used, this time occurred at the end of the run since method V gave the best agreement with method I at that location. Theoretically, if a temperature nearer the heated surface had been used, the time of evaluation would be later since the slope is higher at a given time and vice versa. Therefore, the following observations may be made about method V:

(1) Determination of $\dot{q}$ requires only one thermocouple. However, the time at which $\partial t/\partial\theta$ is taken to give a realistic value of $\dot{q}$ must be determined by some other method.

(2) The transient heat transfer $\dot{q}$ has little significance; and, if h is to be determined, several thermocouples are required to obtain the approximate wall temperature by extrapolation unless a thermocouple can be located on the heat-transfer surface of the plug.

Method VI

The semilog extrapolation method makes use of the assumption that log t plotted against distance is linear through the two innermost temperature readings to the wall. If this is true, the slope $\partial t/\partial x$ at the wall and t_w is determined, from which h may be calculated if t_r is known. The following statements may be made about method VI:

(1) At least two thermocouples must be used, and they should be close to the inner wall.

(2) Small errors in the slope and temperature values at the wall result in relatively large errors in calculated values of h.

CONCLUDING REMARKS

It has been shown that quasi-steady-state, gas-side heat-transfer coefficients may be determined from transient one-dimensional temperature data with small error over an appreciable range of wall temperature. The data were analyzed by six selected methods to obtain the surface heat-transfer coefficient h. To apply these methods to the data, it is generally necessary to obtain short, smooth transitions to stable operating conditions. Insulating all surfaces of the plug except the heat-transfer surface helps to achieve local, one-dimensional conditions and also improves the accuracy of application of the methods to the data.

In the determination of local heat-transfer coefficients based on experimental results obtained from an ammonia-oxygen rocket, the following statements can be made:

1. Methods I to V give comparable values of h near the end of burning time for both chamber and throat tests.

2. Method I (integration) is reasonably easy to apply and is particularly good when running times are short.

3. Method II (constant h) is probably the easiest of all to apply and is particularly good when running times are long. It requires the use of only one thermocouple.

4. The derivation of method III (Cresci-Libby) is rigorous but is the most difficult to apply.

5. Method IV (numerical) is less accurate than methods I and II.

6. The accuracy of methods I to IV may be affected by the starting transient, but this effect decreases with burning time.

7. Method V (Greenfield) agrees well with methods I to IV at the end of burning, but some technique is required to select the time at which to determine $dt/d\theta$ and t_w at a fixed value of x/L.

8. Method IV (semilog extrapolation) is too inaccurate for this type of application.

Lewis Research Center
National Aeronautics and Space Administration
Cleveland, Ohio, January 20, 1960

APPENDIX - SYMBOLS

A	area, sq in.
c	specific heat at constant pressure, Btu/(lb)(°F)
D	diameter, in. (fig. 9)
f	function
h	surface coefficient of heat transfer, Btu/(sq in.)(sec)(°F)
k	thermal conductivity, Btu/(in.)(sec)(°F)
L	length of plug, in.
Q	quantity of heat, Btu/cu in.
$\dot{q}$	quantity of heat per unit area per unit time, Btu/(sec)(sq in.)
r	recovery factor
t	temperature, °F
W	weight of plug, lb
x	distance normal to the heated surface, in.
α	thermal diffusivity, sq in./sec
θ	burning time, sec
λ	integration variable, time
ρ	density, lb/cu in.
φ	surface temperature function

Subscripts:

a	average
o	temperature of solid at zero burning time
r	recovery
s	static

t	total
w	wall
x	distance
θ_1, θ_2	time
0	cold end of plug
1	location of (2/3L) (see fig. 9)

REFERENCES

1. Staff of Rohm & Haas Company: Quarterly Progress Report on Weapons Research, Dec. 15, 1956 to Mar. 15, 1957. Rep. P-57-5, Redstone Arsenal Res. Div., Rohm & Haas Co., Apr. 10, 1957.

2. Carslaw, H. S., and Jaeger, J. C.: Conduction of Heat in Solids. Univ. Press (Oxford), 1950.

3. Gordon, Sanford, and Glueck, Alan R.: Theoretical Performance of Liquid Ammonia with Liquid Oxygen as a Rocket Propellant. NACA RM E58A21, 1958.

4. Eckert, E. R. G.: Introduction to the Transfer of Heat and Mass. McGraw-Hill Book Co., Inc., 1950.

5. Hatch, James E., Schacht, Ralph L., Albers, Lynn U., and Saper, Paul B.: Graphical Presentation of Difference Solutions for Transient Radial Heat Conduction in Hollow Cylinders with Heat Transfer at the Inner Radius and Finite Slabs with Heat Transfer at One Boundary. NASA TR R-56, 1959.

6. Storm, M. L.: Heat Conduction in Simple Metals. Jour. Appl. Phys., vol. 22, no. 7, July 1951, pp. 940-951.

7. Cresci, Robert J., and Libby, Paul A.: Some Heat Conduction Solutions Involved in Transient Heat Transfer Measurements. TN 57-236, WADC, Sept. 1957. (Contract AF-33(616)-3265.)

8. Jakob, Max: Heat Transfer. Vol. 1. John Wiley & Sons, Inc., 1949.

9. Greenfield, Stanley: Determination of Rocket-Motor Heat-Transfer Coefficients by the Transient Method. Jour. Aero. Sci., vol. 18, no. 8, Aug. 1951, pp. 512-518; 526.

10. McAdams, William H.: Heat Transmission. Second ed., McGraw-Hill Book Co., Inc., 1942.

TABLE I. - VALUES OF SURFACE HEAT-TRANSFER COEFFICIENT ANALYZED BY SIX METHODS

Location	Method	Time, sec	Heat-transfer coefficient, Btu/(sec)(sq in.)(°F)	Percent variation from method I (integration), eq. (2a)
Chamber	I: Integration	2.1		
	Eq. (2a)		0.00176	
	Eq. (2b)		.00160	-9
	II: Constant h			
	Time measured from initiation of propellant flow		.00176	0
	III: Cresci-Libby		.00204	16
	IV: Numerical		.00189	7
	V: Greenfield		.00172	-2
	VI: Semilog extrapolation		.00216	23
Throat	I: Integration	2.5		
	Eq. (2a)		0.00286	
	Eq. (2b)		.00251	-12
	II: Constant h			
	Time measured from initiation of propellant flow		.00253	-12
	Time measured 0.6 sec after initiation of propellant flow		.00284	-1
	III: Cresci-Libby		.00263	-7
	IV: Numerical		.00293	2
	V: Greenfield		.00266	-7
	VI: Semilog extrapolation		.00335	17

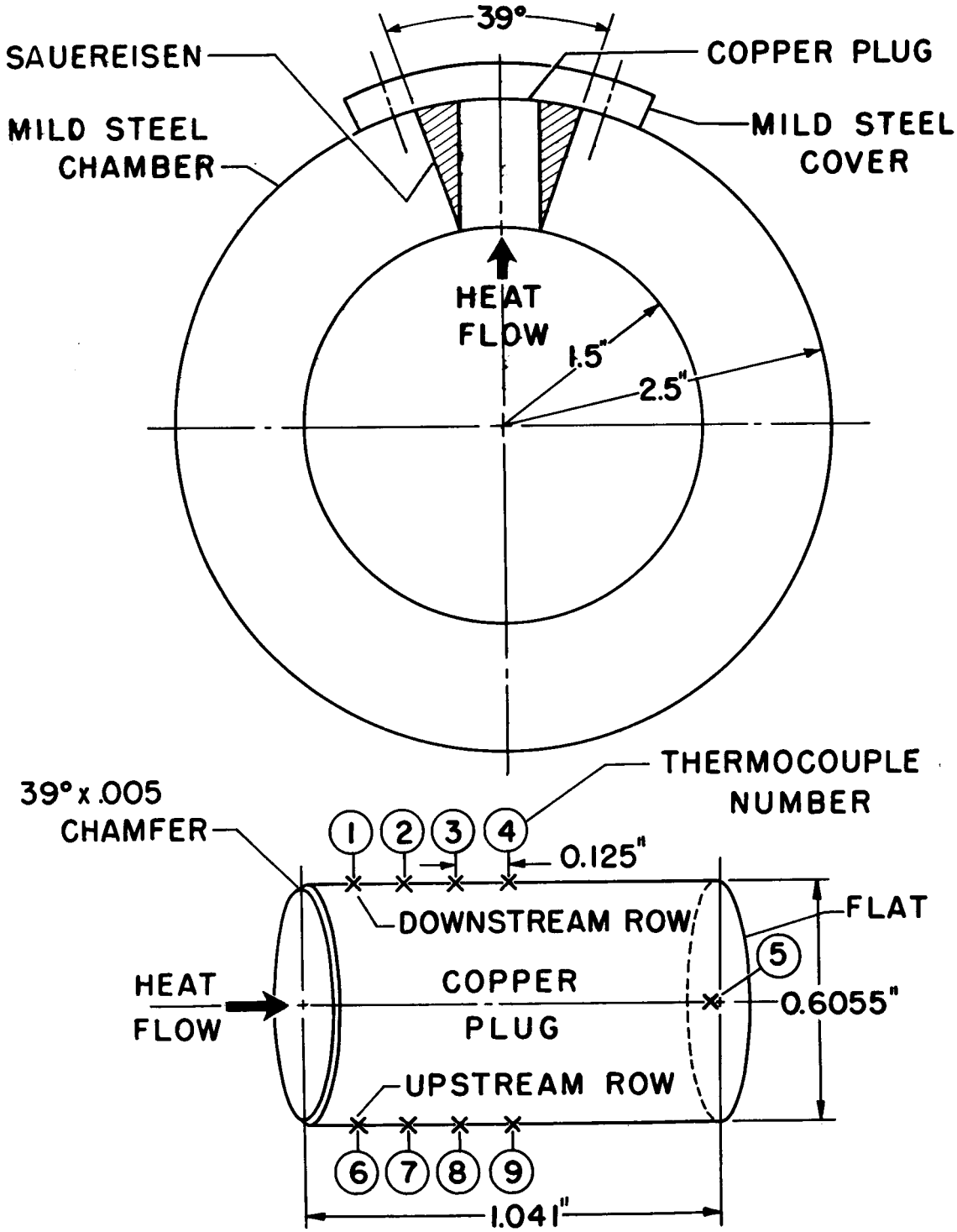

Figure 1. - Installation of copper plug in rocket chamber wall.

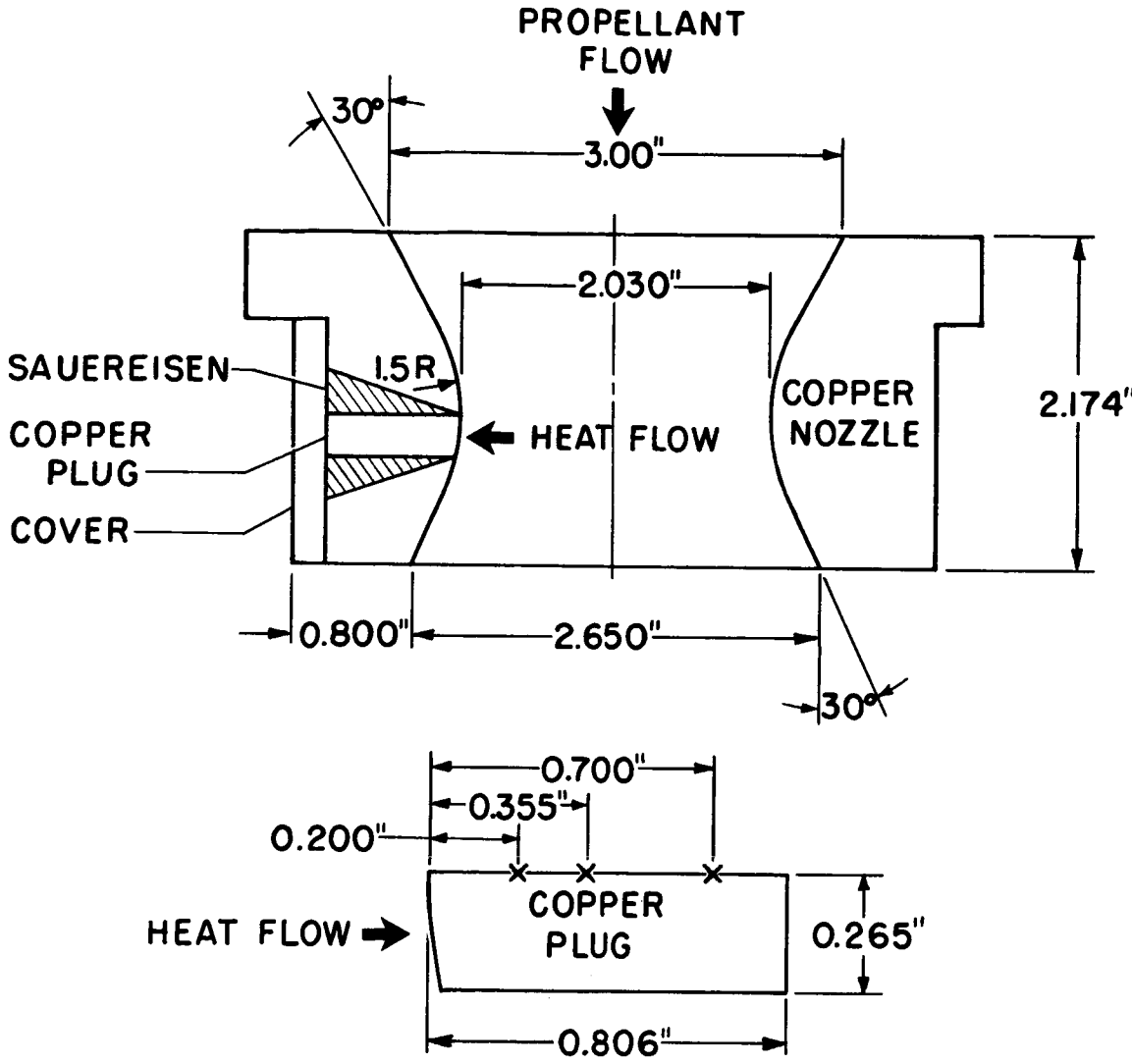

Figure 2. - Installation of copper plug in rocket nozzle wall.

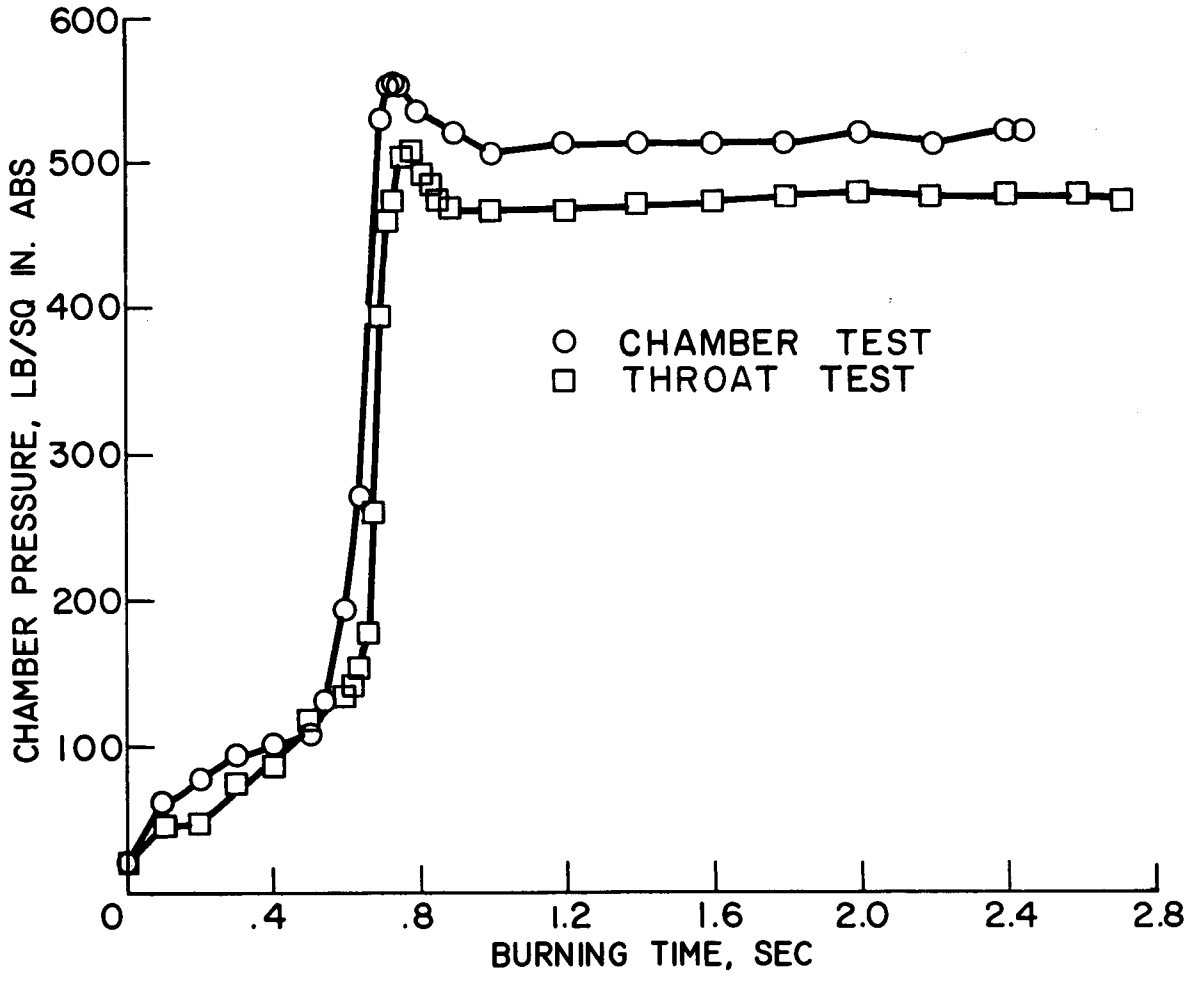

Figure 3. - Variation of chamber pressure with burning time.

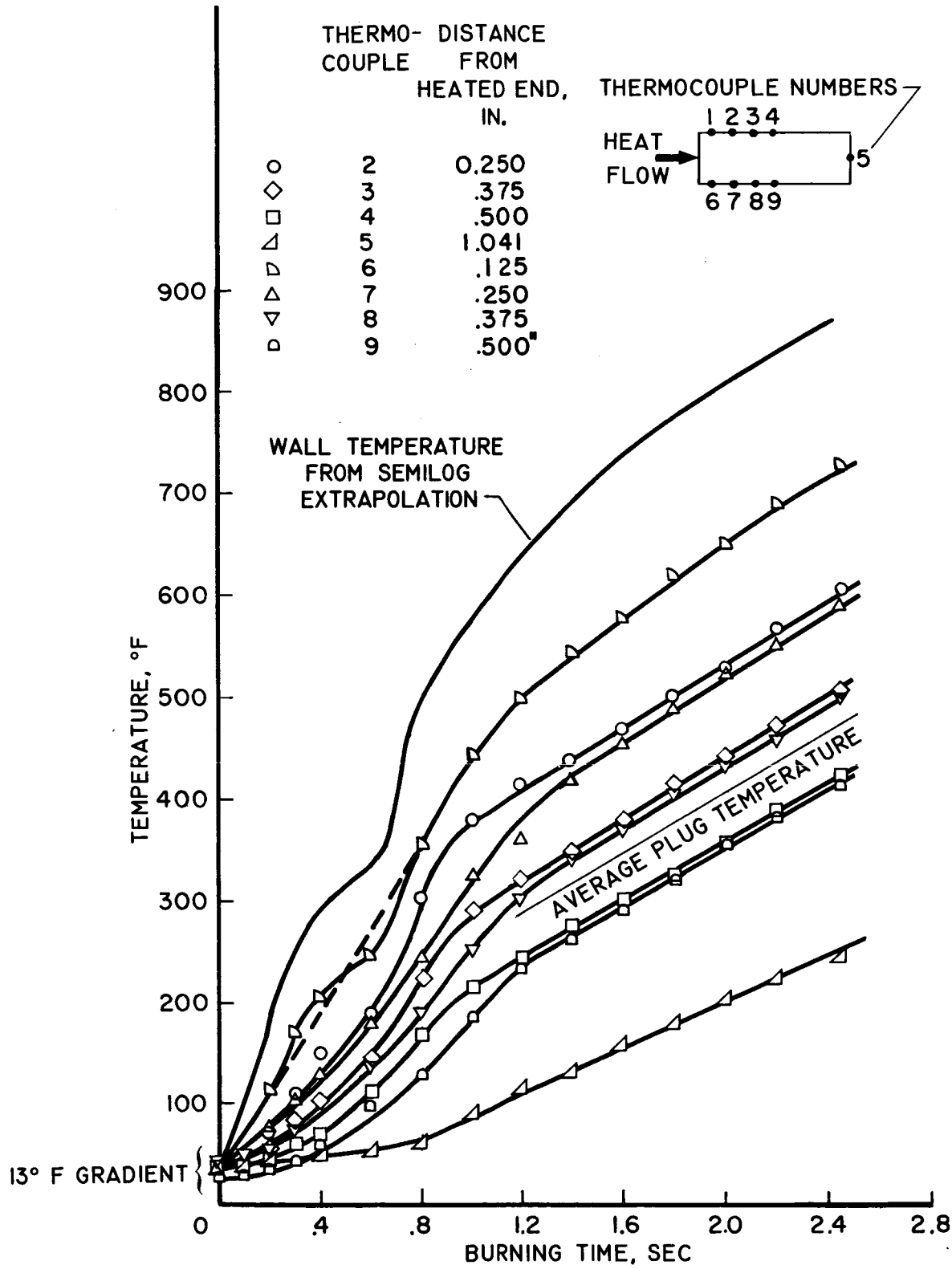

Figure 4. - Variation of temperature with burning time for chamber plug.

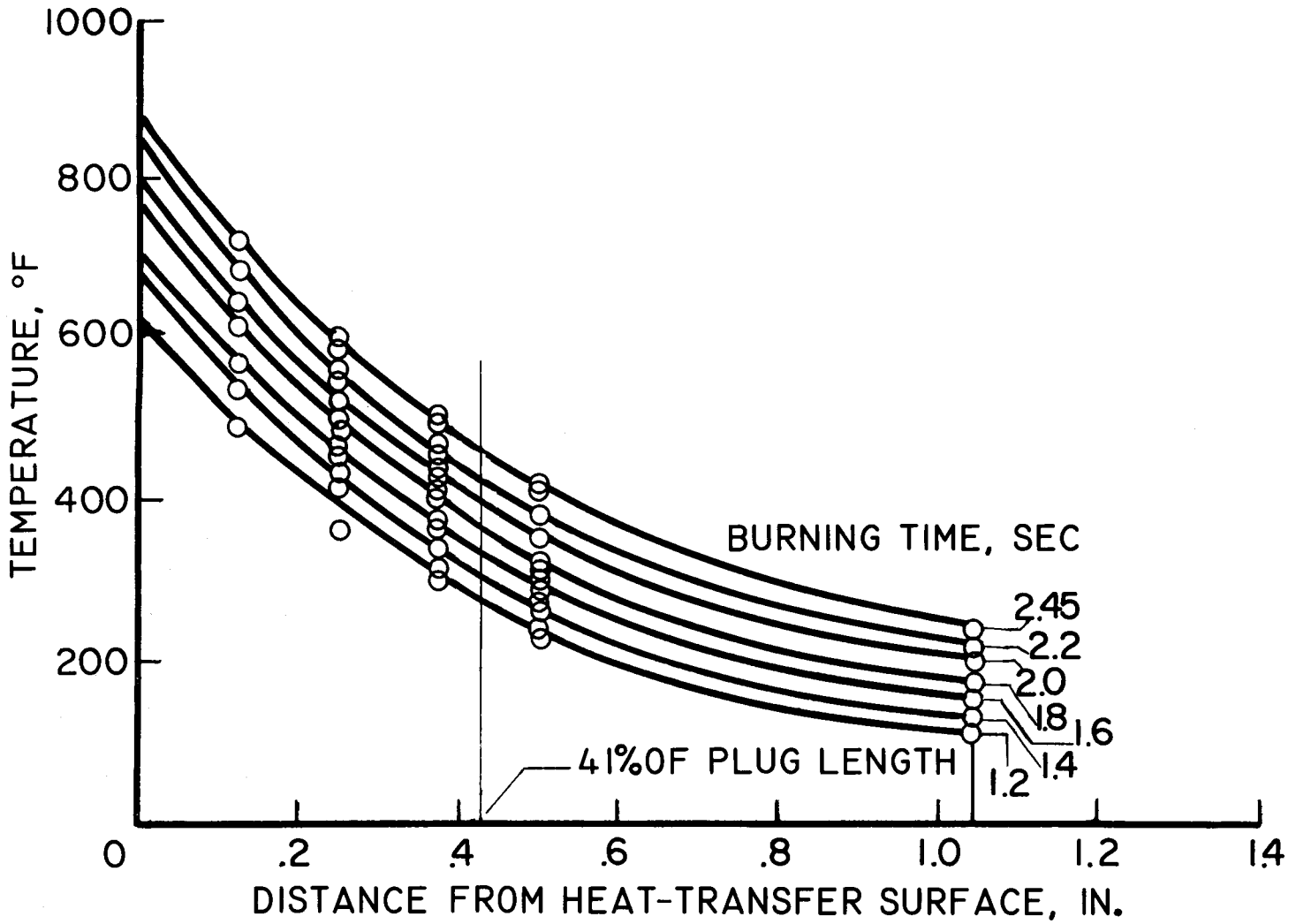

Figure 5. - Variation of temperature with plug length for chamber plug.

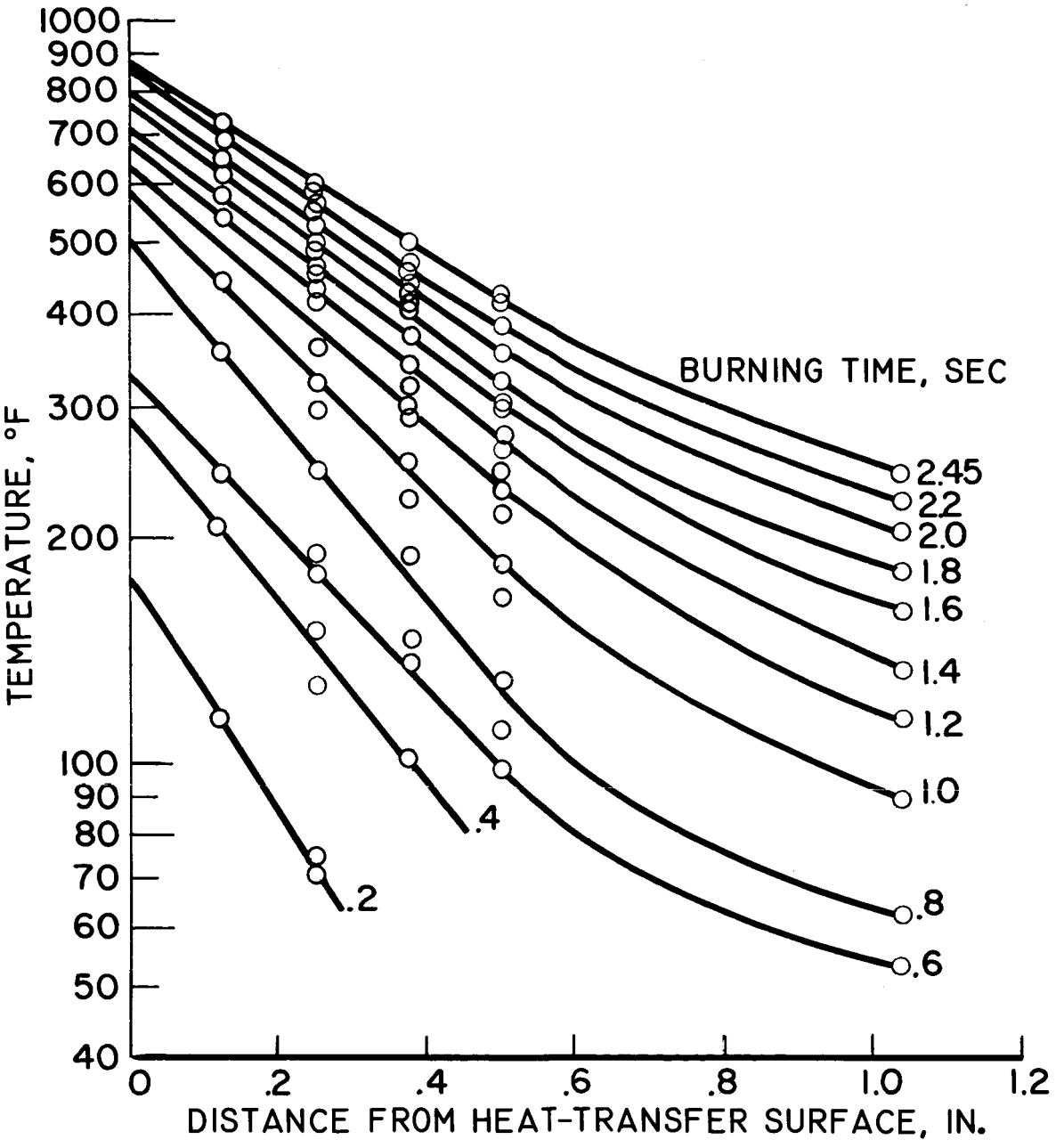

Figure 6. - Semilog plot of variation of temperature with plug length for chamber plug.

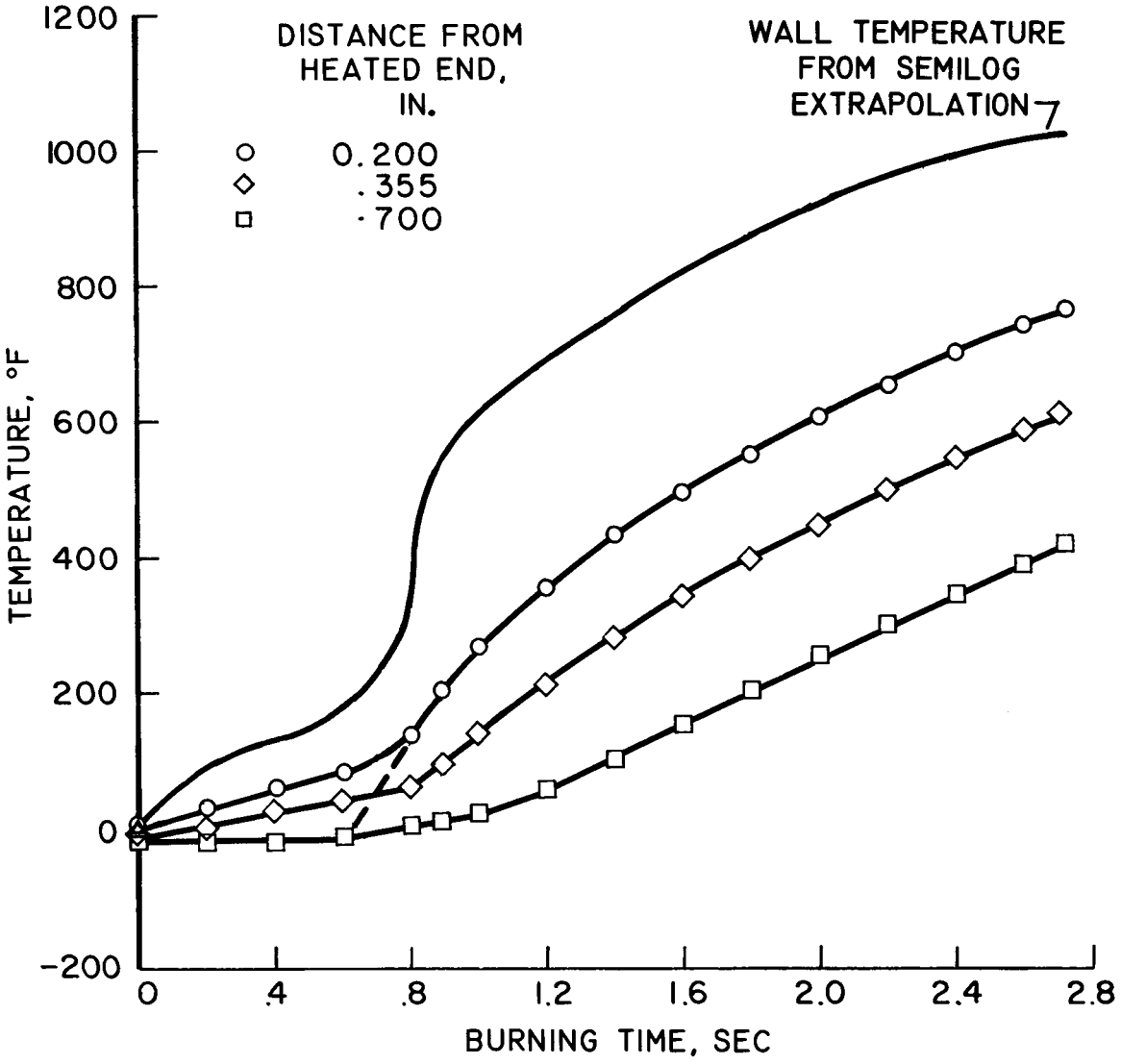

Figure 7. - Variation of temperature with burning time for nozzle plug.

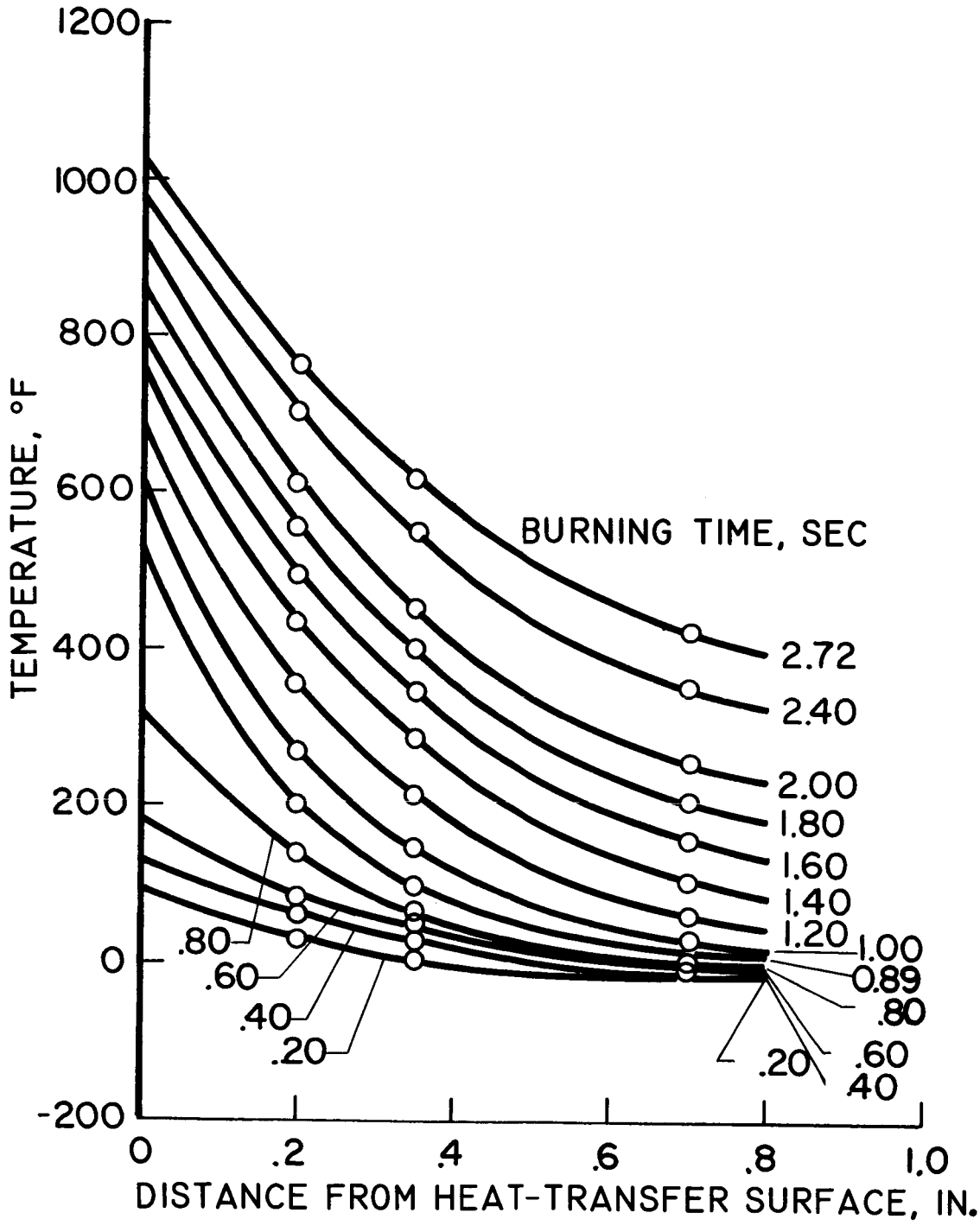

Figure 8. - Variation of temperature with plug length for throat plug.

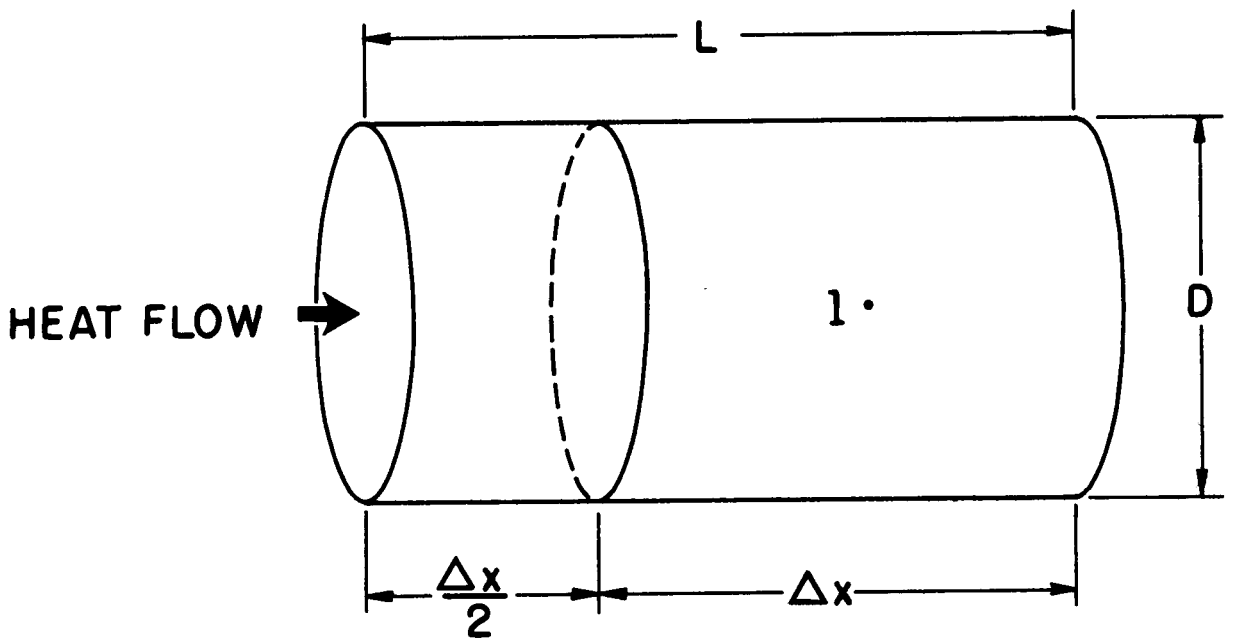

Figure 9. - Configuration used for determination of heat-transfer coefficient in method IV (numerical).

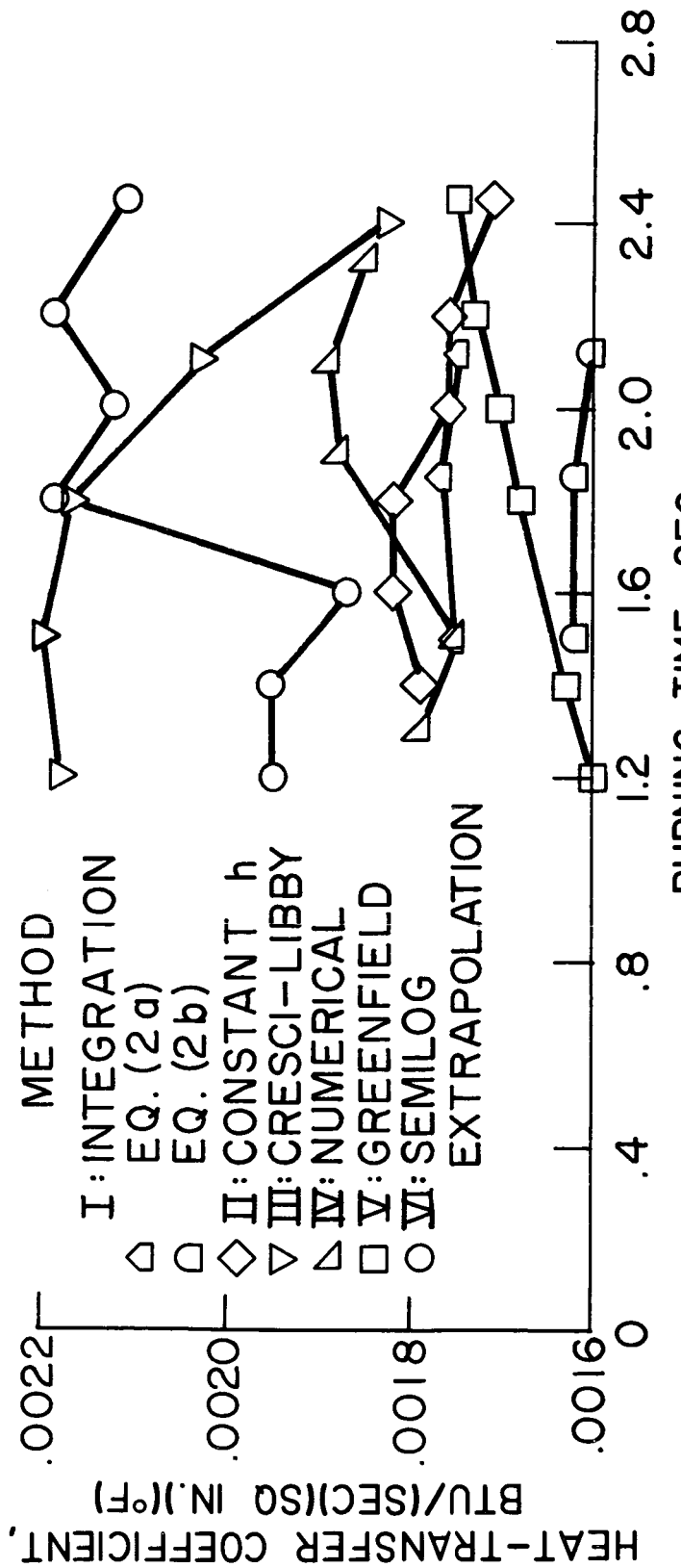

Figure 10. - Comparison of h in chamber.

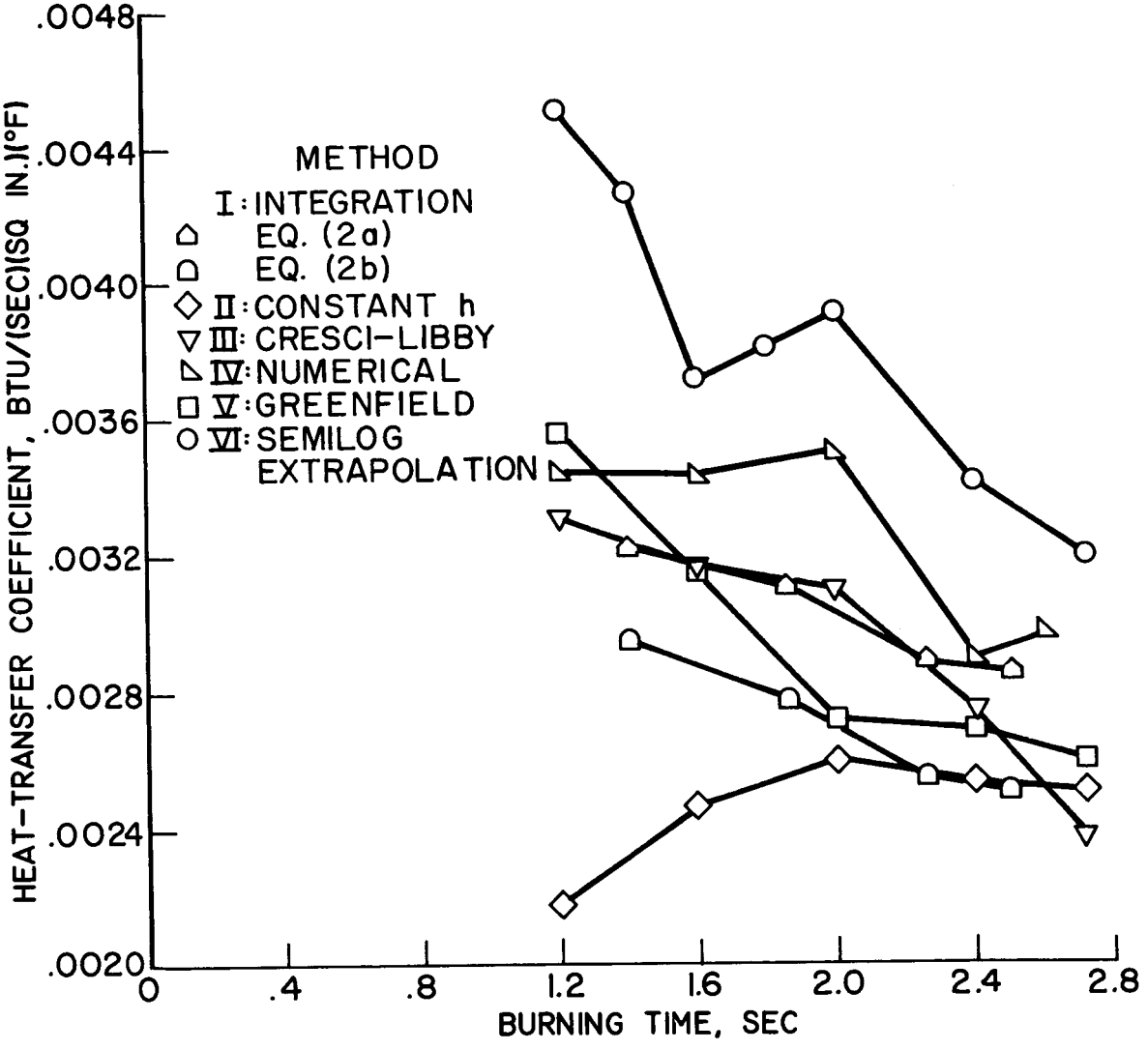

Figure 11. - Comparison of h in throat.

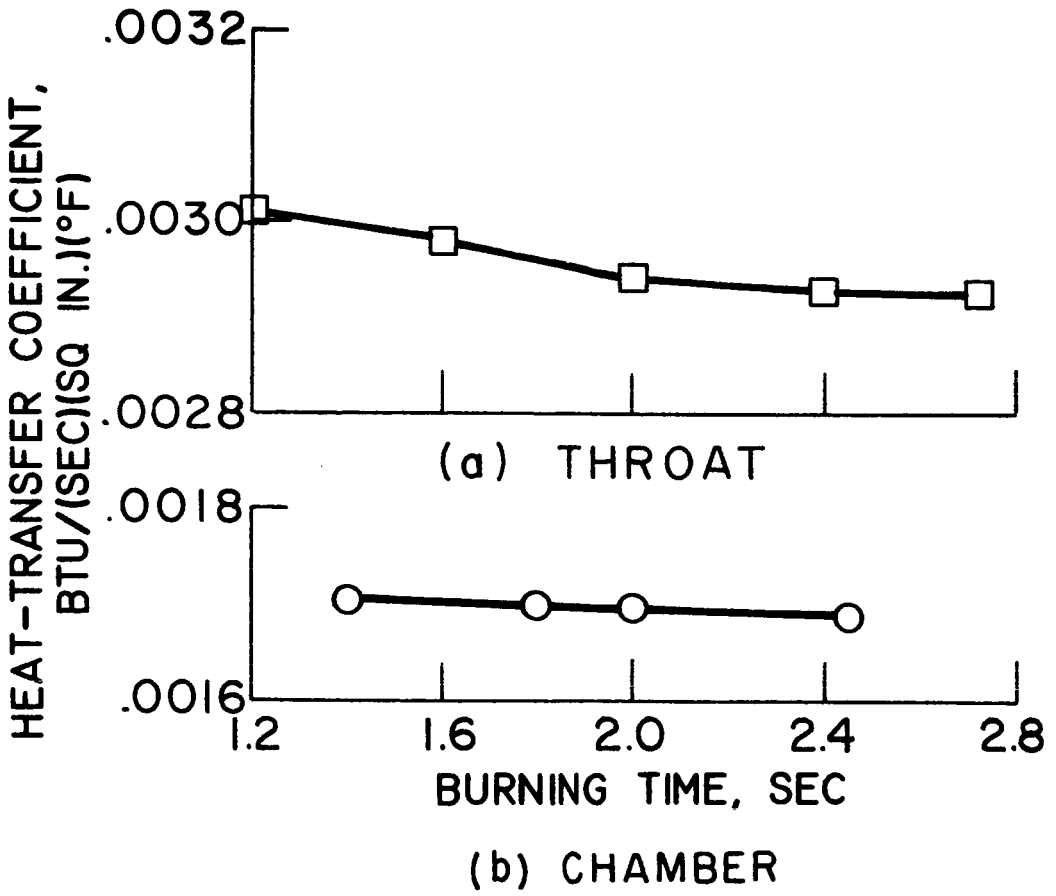

Figure 12. - Variation of h computed from Colburn equation in chamber and throat.